Measuring Vesicle Loading with Holographic Microscopy and Bulk Light Scattering: Supporting Information

Lan Hai Anh Tran,[†,#] Lauren A. Lowe,[†,‡,#] Yaam Deckel,[†,‡] Matthew Turner,[†,¶] James Luong,[†,§] Omar Abdullah A Khamis,[†] Megan L. Amos,[†,‡] and Anna Wang[*,†,‡,‖,⊥]

†*School of Chemistry, UNSW Sydney, NSW 2052, Australia*

‡*Australian Centre for Astrobiology, UNSW Sydney, NSW 2052, Australia*

¶*School of Physics, The University of Sydney, NSW 2006, Australia.*

§*School of Chemistry, The University of Sydney, NSW 2006, Australia.*

‖*ARC Centre of Excellence in Synthetic Biology, UNSW Sydney, NSW 2052, Australia*

⊥*RNA Institute, UNSW Sydney, NSW 2052, Australia*

#*These authors contributed equally*

E-mail: anna.wang@unsw.edu.au

Video S1 The intensity values across the centre of the hologram are shown for vesicles with varying radii r. Other parameters: $z = 10$ μm, the internal refractive index $n = 1.35$, the lipid refractive index $n_{lipid} = 1.47$, and the lipid shell thickness $t = 3$ nm.

Video S2 The intensity values across the centre of the hologram are shown for vesicles with varying z. Other parameters: $r = 1$ μm, $n = 1.35$, $n_{lipid} = 1.47$, and $t = 3$ nm.

Video S3 The intensity values across the centre of the hologram are shown for vesicles of varying internal refractive index n. Other parameters: $r = 1$ μm, $z = 10$ μm, $n_{lipid} = 1.47$, and $t = 3$ nm.

Video S4 The data holograms for the vesicle sample corresponding to Figure 4 are shown. Holograms for the vesicles of interest at each slice were analyzed to yield Figure 4C.

Additional figures

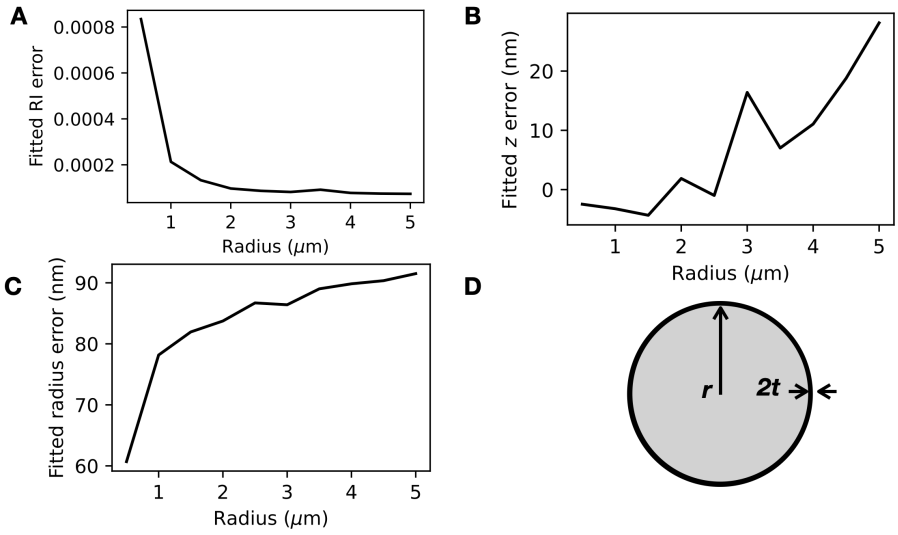

Figure S1: The light scattering model for a homogeneous sphere is used to extract the refractive index of the contents of a bilamellar vesicle (a core-shell scatterer with a very thin shell consisting of two lipid bilayers). **A.** The fitted error in the refractive index n decreases dramatically for vesicles larger than 1 μm in radius. **B.** The fitted error in z fluctuates with vesicle size. **C.** The fitted error in r is approximately 90 nm for all vesicle sizes. **D.** A schematic showing a core-shell scatterer with inner radius r and shell thickness $2t$.

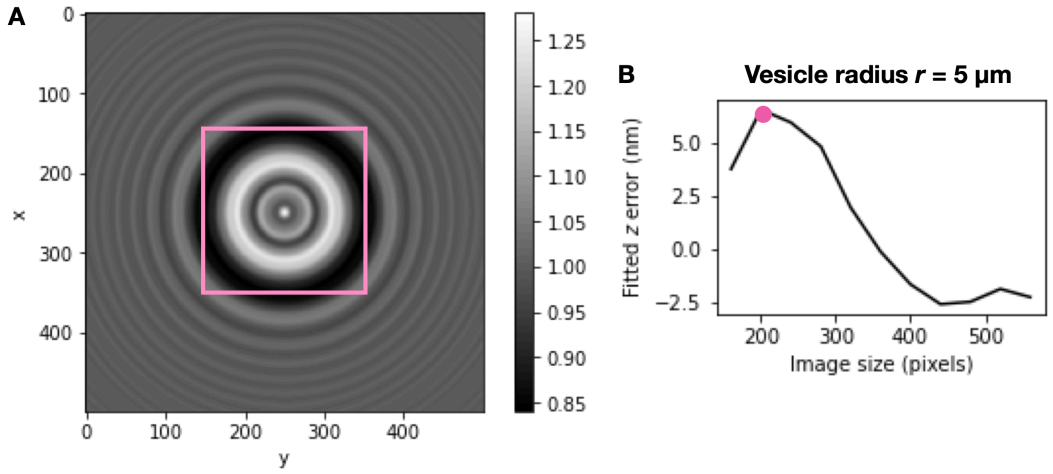

Figure S2: **A.** The analyzed image size can be varied. The pink box delineates a 200 pixel × 200 pixel box. **B.** For larger vesicles, the error in fitted z decreases with hologram image size. The pink box in **A** corresponds to the pink dot in **B**.

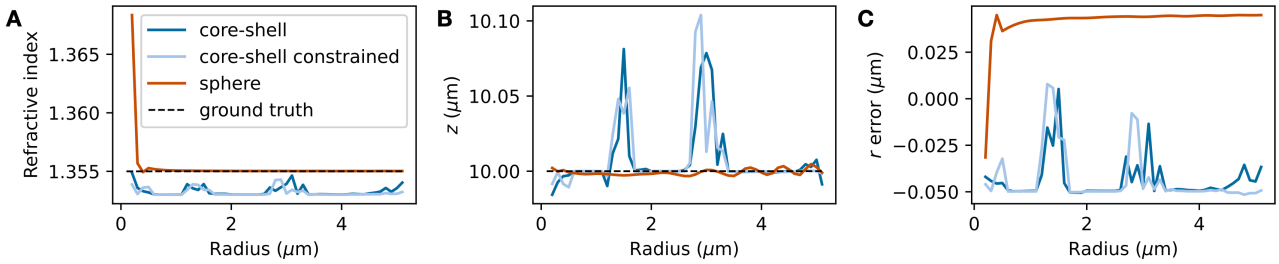

Figure S3: Core-shell holograms were generated in HoloPy for a range of r at a fixed distance of $z = 10$ μm. Three models were then used to fit the hologram: a core-shell model with no constraints for the shell thickness or refractive index; a core-shell model with constraints for the shell thickness (between 2.99–3.01 nm, uniform prior) or refractive index (between 1.4663–1.4665, uniform prior). The initial guesses for fitting were exact for all parameters except n, which was 0.002 smaller than the ground truth refractive index of the contents, and r, which was 50 nm smaller than the ground truth radius. **A.** Except for vesicles smaller than 1 μm in radius, the sphere model performed exceptionally well for retrieving the refractive index of the vesicle contents. **B.** The optimizer for the core-shell models became trapped in local minima for the z values that deviated from the ground truth. **C.** The initial guess for r being 50 nm smaller than the ground truth appears to lead the optimizer into being trapped in local minima for the core-shell models, but not the effective sphere model.

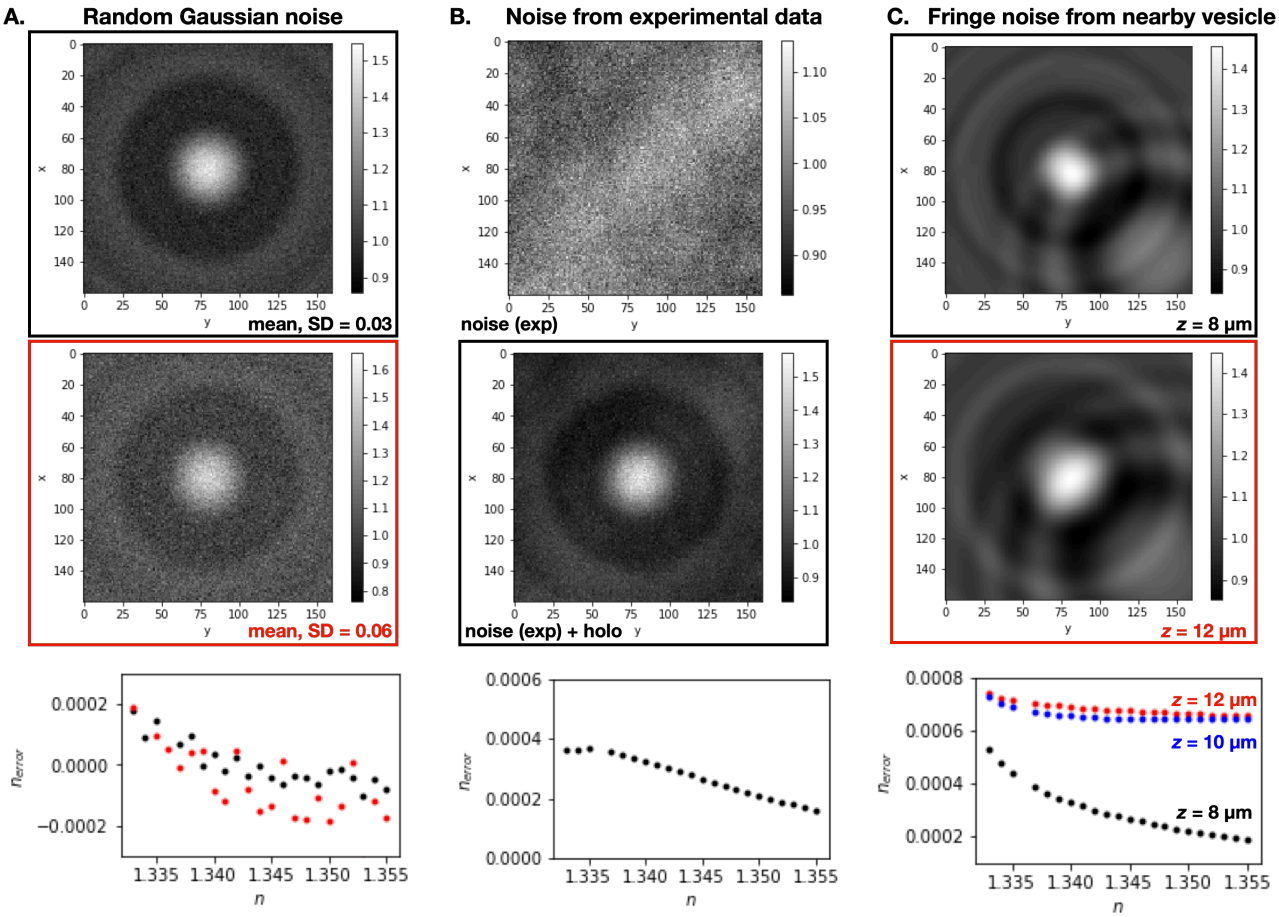

Figure S4: Holograms of vesicles in water are simulated using a core-shell model for contents of varying refractive indices n, then retrieved with a sphere model. Values used: $r = 1.5$ μm, $n_{water} = 1.331$, $z = 10$ μm, lipid refractive index $n_{lipid} = 1.47$, and the lipid shell thickness $t = 3$ nm. **A.** Random Gaussian noise with standard deviation (SD) and mean both set to 0.03 (black) or 0.06 (red) added to the hologram do not compromise the retrieved refractive index by more than 0.0002 RIU, even for n close to n_{water}. **B.** Noise, taken from typical experimental data, consists of both random noise and background variations. For a simulated hologram that has this experimental noise added to it, the noise does not compromise the retrieved refractive index by more than 0.0004 RIU, even for n close to n_{water}. **C.** A second vesicle ($r = 0.75$ μm, $n = 1.353$, lipid refractive index $n_{lipid} = 1.47$, and lipid shell thickness $t = 3$ nm) is introduced nearby and situated 5 μm further from the focal plane than the first vesicle. The impact of the second vesicle on the retrieved n for the central vesicle is shown for different z distances for the central vesicle. The error changes with z and is larger for more weakly-scattering central vesicles.

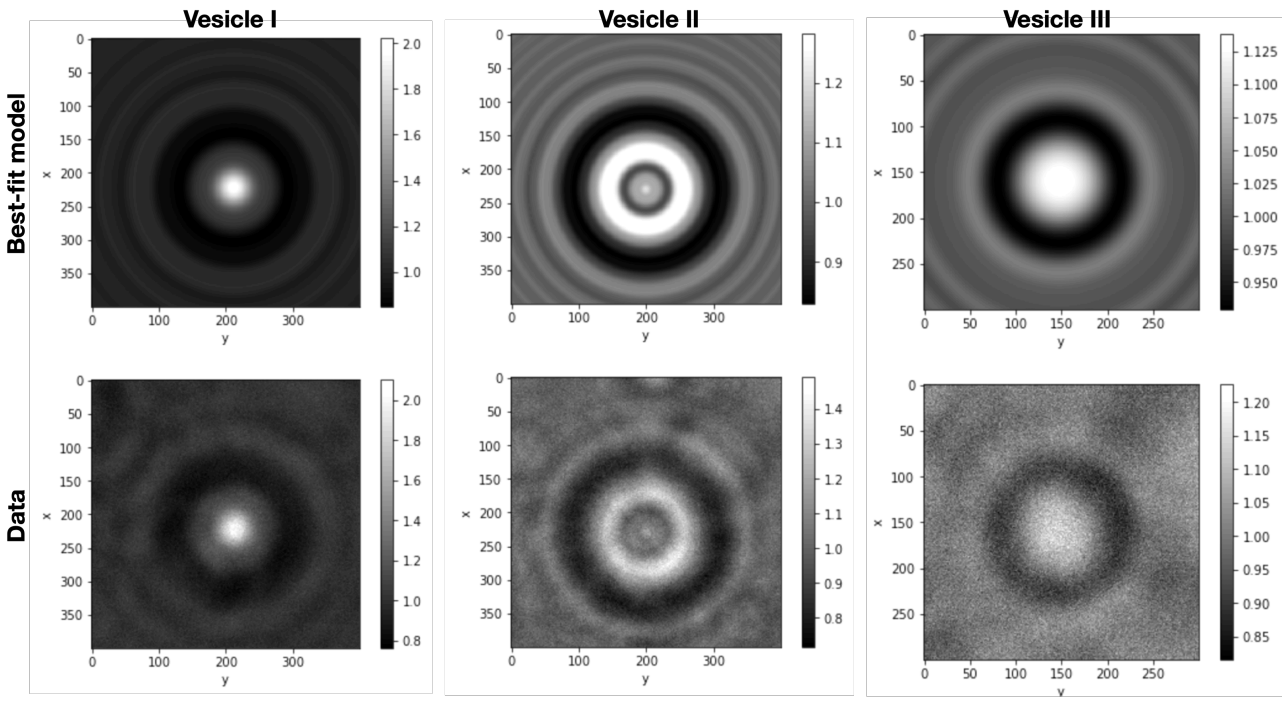

Figure S5: Examples of data holograms and best-fit holograms of three vesicles. x and y dimensions are in pixels.

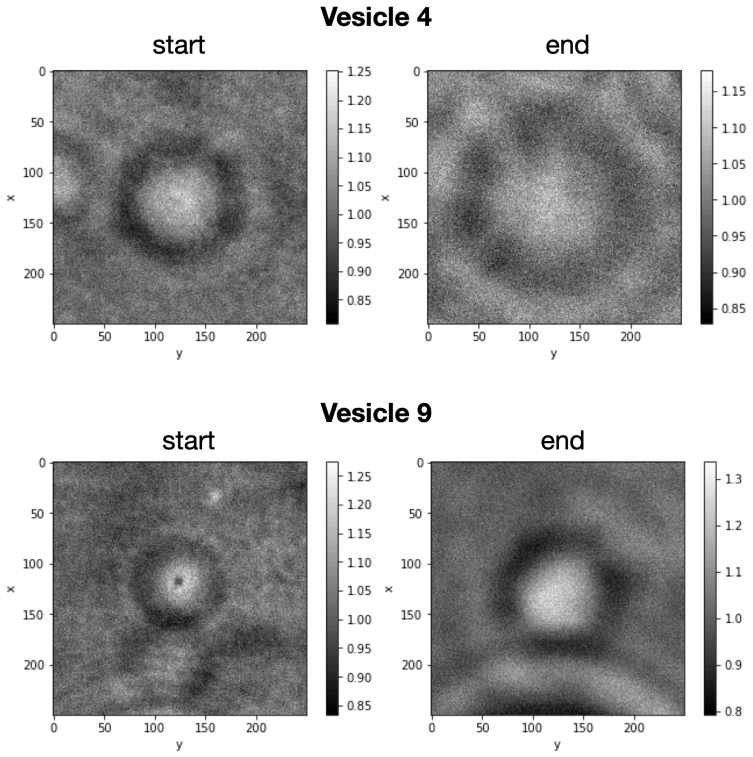

Figure S6: Holograms of vesicles 4 and 9 show fringes from neighboring vesicles throughout the whole dataset from Figure 4.

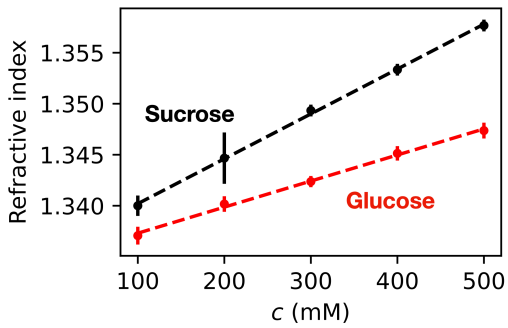

Figure S7: The average measured refractive indices at 589 nm for sucrose and glucose solutions that also contain 100 mM bicine (pH 8.3) are shown. Error bars represent the standard deviation from the mean ($N = 3$ for each data point). Lines of best fit are shown as dotted lines. For sucrose, the slope is 4.400 $\times 10^{-5}$. For glucose, the slope is 2.557 $\times 10^{-5}$.

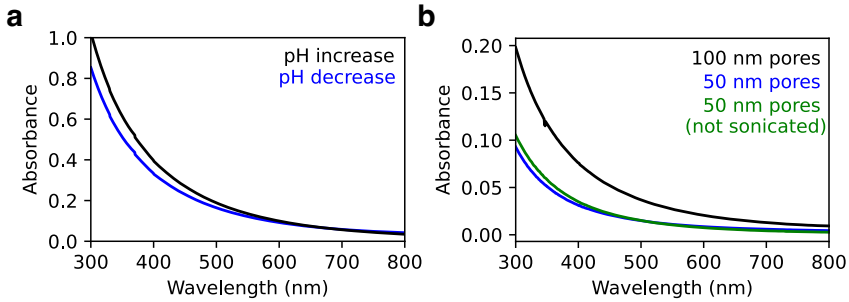

Figure S8: Vesicle preparation method impacts bulk sample scattering. (a) 10 mM OA vesicles prepared by increasing the pH of oleic acid (black, pH 8.40) scatter more light than vesicles prepared by decreasing the pH of oleate micelles (blue, pH 8.48), likely owing to vesicles prepared from micelles being more unilamellar and a change in the pH-dependent properties of fatty acid vesicles.[1] (b) When prepared via thin-film hydration, 1 mM POPC vesicles that are sonicated and then extruded through 50 nm pores (blue) scatter less light than samples that are extruded without sonication (green). Samples sonicated and extruded through 100 nm pores (black) scatter significantly more light than samples extruded through 50 nm pores.

Further Methods

Oleic acid vesicle samples in Figure S8 were prepared via a pH decrease or increase method. The pH decrease method is similar to the procedure described in the main text, with 100 mM oleate micelles first prepared. The pH was decreased by adding 100 μL of 100 mM oleate micelles to a solution containing 200 μL of 1 M Na-bicine (pH 8.5) and 700 μL of Milli-Q water to yield a sample of 10 mM oleic acid vesicles in 200 mM Na-bicine. The sample was left to agitate on an orbital shaker overnight (PSU-10i Grant Bio, UK) at 110 rpm.

For the pH increase method, 100 μmoles of neat oleic acid was added to a 1 mL solution containing 200 mM Na-bicine (pH 8.5) and 50 mM NaOH. The solution was left to agitate on an orbital shaker overnight (PSU-10i Grant Bio, UK) at 110 rpm. The vesicles were then diluted into a dilution buffer containing 200 mM Na-bicine to a final concentration of 10 mM oleic acid.

Using a mini-extruder (Avanti Polar Lipids, USA), samples made using both methods were extruded 21 times through a polycarbonate membrane with pores 100 nm in diameter.

The POPC vesicle sample extruded through 100 nm pores in Figure S8 (black) was prepared as described in the main text. The sample extruded through 50 nm pores (blue) was prepared in the same way, with only the pore size of the polycarbonate extrusion membrane differing. The non-sonicated sample was also extruded through 50 nm pores, but the sample was not sonicated before extrusion, and the POPC was initially dissolved in ethanol rather than chloroform for the preparation of the thin film. After extrusion, all samples were diluted 1 in 10 into an isotonic dilution buffer containing 1x PBS and 500 mM sucrose (pH 7.4).

References

(1) Lowe, L. A.; Kindt, J. T.; Cranfield, C.; Cornell, B.; Macmillan, A.; Wang, A. Subtle changes in pH affect the packing and robustness of fatty acid bilayers. *Soft Matter* **2022**, *18*, 3498–3504.